agronomy

MDPI

Article

DEM-MBD Coupling Simulation and Analysis of the Working Process of Soil and Tuber Separation of a Potato Combine Harvester

Yuyao Li [1], Zhichao Hu [1], Fengwei Gu [1], Bing Wang [1], Jiali Fan [1], Hongguang Yang [1,*] and Feng Wu [2,*]

[1] Nanjing Institute of Agricultural Mechanization, Ministry of Agriculture and Rural Affairs, Nanjing 210014, China; l598658625@163.com (Y.L.); huzhichao@caas.cn (Z.H.); gufengwei@caas.cn (F.G.); wangbing@caas.cn (B.W.); fjl985144132@163.com (J.F.)

[2] Graduate School of Chinese Academy of Agricultural Sciences, Beijing 100083, China

* Correspondence: hgyang2016@163.com (H.Y.); xuefeng_1223@163.com (F.W.)

Abstract: To address the competing relationship between tuber damage and soil removal in potato combine harvesting, this study investigated the operating mechanism of a belt-rod type separator of a small-scale self-propelled potato combine harvester and the separation performance between tuber and soil. The main factors affecting the tuber-soil separation characteristics were derived from a theoretical analysis of the belt-rod angle, belt-rod linear velocity, and harvester forward speed. A simulation model based on DEM (Discrete Element Method)-MBD (Multibody Dynamics) coupling was constructed and single-factor simulation tests were carried out. Then a three-factor, three-level Box–Behnken test was conducted using the coefficient of force on the tuber and soil clearing rate as response indicators. The optimal combination of parameters resulting in low tuber damage and high soil clearing rate was obtained by solving the regression equations. The optimal parameters were a belt-rod angle of 17.5°, a belt-rod linear velocity of 1.37 m/s, and a harvester forward speed of 0.80 m/s. The simulation model was validated by field experiments and the error between the simulation model and the field harvest was found to be 3.81%. The results can be used as a reference for parameter optimization of small-scale potato combine harvesters and coupled DEM-MBD simulation of tuber-soil separation.

Keywords: potato; combine harvester; separation of tuber and soil; tuber damage; coupling model of DEM with MBD

Citation: Li, Y.; Hu, Z.; Gu, F.; Wang, B.; Fan, J.; Yang, H.; Wu, F. DEM-MBD Coupling Simulation and Analysis of the Working Process of Soil and Tuber Separation of a Potato Combine Harvester. *Agronomy* **2022**, *12*, 1734. https://doi.org/10.3390/agronomy12081734

Academic Editors: Hua Li and Lizhang Xu

Received: 16 June 2022
Accepted: 20 July 2022
Published: 22 July 2022

1. Introduction

The potato is strategically important as the fourth non-grain food crop in China [1]. The full mechanization of the potato industry has received a lot of attention, and potato harvesting has a large impact on potato yields and varieties. It is necessary to improve the potato machinery harvesting capacity and harvesting efficiency. The improvement of soil-tuber separation is the key to potato harvest quality, so it is worth considering how to improve the separation of the soil while reducing the damage to the potato tuber [2–4]. At present, most of the research on tuber-soil separation in China is focused on the potato digger which can only complete the tuber digging and preliminary soil removal, and there is little research on the use of combine harvesters. The requirements for tuber-soil separation also differ between the two methods. The combine harvester can complete the tasks of digging, removing soil, collecting, and bagging at one time. Potato tubers are more likely to be damaged by long contact time with the harvester throughout the combine harvesting process [5,6]. The soil can also be separated in the lifting and haulm removal section. However, the tubers are thrown down into the soil after the tuber-soil separation in the digger. The separation time is short and the requirements for the soil clearing effect

are higher [7,8]. Therefore, the separation of the tuber-soil mixture dug up by the combine harvester should cause as little damage as possible to the potato.

To date, many scholars have carried out theoretical analysis and experimental research on potato mechanical harvesting. AI-Dosary et al. [9] studied the effects of harvester forward speed and digging depth on potato tuber damage through field tests. Zhou et al. [10] designed a self-propelled potato harvester and then carried out a field test of their design. Lv et al. [11] investigated the effect of the structure and operating parameters of the lifting chain on the damage of potato tubers using a test bed. Wu et al. [12] optimized the parameters of a potato digger for sticky soils by artificial feeding. However, most of the research on tuber-soil separation devices in potato harvesting has been realized through field tests or bench tests. Harvester experiments in the field most directly reflect post-harvest tuber damage and residual soil, but it is not easy to study the process of soil sieving and potato damage. Bench tests often focus on the damage to the potato tubers and do not provide an accurate analysis of the separation process of the potato-soil mixture.

In recent years, with the progress of computer technology and the rapid development of the discrete element method, many scholars have used the discrete element method to study and analyze agricultural machinery [13–16]. Studies of mechanical harvesting using the discrete element method are also increasingly being carried out for root crops, edible tubers, and rhizomes. Wei et al. [17] analyzed the influence of the structure and working parameters of the wavy separation on the tuber-soil separation process based on the discrete element method and determined the separation form and the corresponding parameter combinations. Park D. et al. [18] investigated and verified the impact forces on the garlic bulb in the garlic harvester using EDEM software. Both Li et al. [19] and Gao et al. [20] carried out studies of the sweet potato and soil separation process by EDEM software and optimized the parameters. However, most of the above studies were conducted using discrete element simulation only and most of them are for potato diggers. Fewer studies have been conducted on the simulation and parameter optimization of the potato-soil separation process in a combine harvester.

To sum up, there are some reports on the application of discrete element method in the mechanical harvesting of potato, sweet potato, garlic, and other crops, but most of these studies have focused on small diggers, and the research on combined harvesting has not been reported. This study selected a small-scale self-propelled potato combine harvester as a prototype, and the belt-rod type tuber-soil separator as the research object and then performed a simulation of and research into the tuber-soil separation characteristics in the combined harvesting process. Theoretical analyses of the movement of the rod during operation and the separation of the tuber-soil mixture on the separation mechanism were conducted. The factors affecting the tuber-soil separation characteristics of potato combine harvesters of the belt-rod type were determined. The stress on the potato tuber at harvest and the effect of soil clearing were used as response indicators. A simulation model with EDEM-RecurDyn coupling studying the effect of the belt-rod angle, belt-rod linear velocity, and harvester forward speed on the tuber-soil separation effect was constructed. The optimal set of parameters was derived by the Box–Behnken design test. This paper investigates the characteristics of tuber-soil separation in a combine harvester, which can also provide support for the future optimization of the structure form and operating parameters of the separation device of the small-scale self-propelled potato combine harvester.

2. Structure Principle of Belt-Rod Type Separator and Its Layout in the Whole Harvester

2.1. Structure Principle of Belt-Rod Type Separator

The main function of the belt-rod type separator is to separate the soil in the tuber-soil mixture transported by the digging shovel. The main components are a frame, support belt pulleys, rods, a drive shaft, and jockey pulleys, as shown in Figure 1. The rods

are fastened directly to the belts by rivets. The upper pulley supports the belt so that there is an angle difference (β) between the front and rear belt-rod. The plum-shaped wheel on the drive shaft engages with the rod and drives the belt-rod. During the harvesting operation, the excavated mixture consists of three main components: fine grain soil, large soil blocks and potato tubers. When transported to the separator, most of the fine grain soil is sieved out and the potato pieces and larger soil pieces move with the rods. With the vibration, collisions and jumping, large soil blocks, as well as soil attached to the surface of tubers, fall off and are separated; the rest of the potatoes and soil blocks are then transported to the subsequent process.

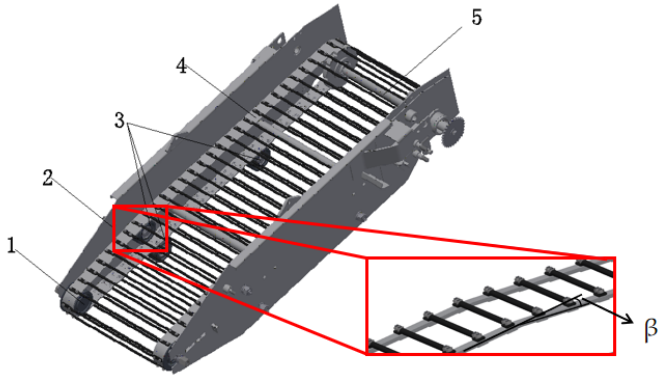

Figure 1. 3D model of belt-rod type potato soil separator: 1-support belt pulley; 2-frame; 3-jockey pulley; 4-rod; 5-drive shaft.

2.2. Layout of the Separator in the Whole Harvester

The small-scale self-propelled potato combine harvester includes the following main components: crawler type self-propelled chassis, transmission system, frame, depth limiting device, digging mechanism, belt-rod type conveying and separating mechanism, separation mechanism of potato and haulm, arc grid connection mechanism, scraper chain lifting mechanism, cleaning and screening mechanism, soil delivery device, and potato collecting mechanism, as shown in Figure 2. The excavated tuber-soil mixture passes through the belt-rod type separator and completes the first sieving. The lifting conveyor transports the mixture upwards to the cleaning and screening mechanism. After selection, the potatoes enter the collection mechanism for bagging. The belt-rod separator is located behind the digging mechanism and in front of the lifting mechanism, which needs to complete the screening of a large amount of fine grain soil. It transports the potatoes with a small number of soil blocks to the lifting mechanism.

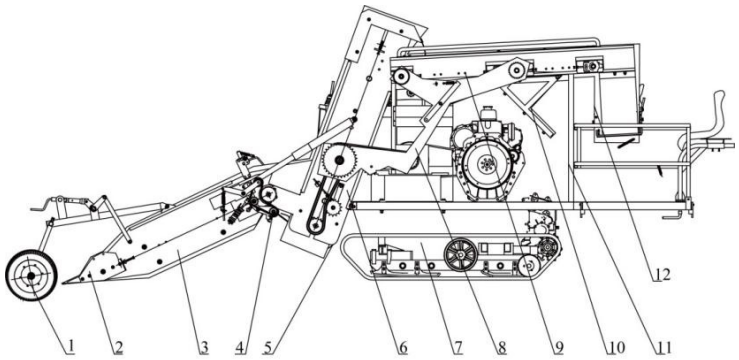

Figure 2. Structure diagram of the small-scale self-propelled potato combine harvester: 1-depth limiting device; 2-digging mechanism; 3-belt-rod type conveying and separating mechanism; 4-separation mechanism of potato and haulm; 5-arc grid connection mechanism; 6-scraper chain lifting mechanism; 7-crawler type self-propelled chassis; 8-transmission system; 9-cleaning and screening mechanism; 10-soil delivery device; 11-frame; 12-potato collecting mechanism.

2.3. The Main Structural Parameters of the Belt-Rod Type Separator

Based on a preliminary study and according to the length requirement of the small-scale potato combine harvester, the length of the separator was determined to be 1450mm. The width was determined to be 560 mm according to the actual ridge shape of potato planting. The general design rod radius is 5–6 mm [21], so 5 mm was selected. According to the shape of the potato, the distance between the rods is 42 mm and the number of teeth of the corresponding plum-shaped wheel is 12.

3. Materials and Methods

3.1. Theoretical Analysis of Potato and Soil Separation Process

3.1.1. Analysis of the Rod Movement

The mechanism is worked by a combination of plum-shaped wheels and belt pulleys. The plum-shaped wheel is the active pulley and the belt pulley is the driven pulley. The running trajectory of one rod during operation can be roughly divided into two sections. The rod comes into contact with the potato-soil mixture and performs sieving operations during the A-B-C section, and during the C-D-E-A section, the rod is unworked. The velocity of the rod (v) can be resolved in the horizontal direction (v_x) and vertical direction (v_y). The speed of the plum-shaped wheel is ω. The angle between the belt-rod and the ground is α. The angle between AB and BC is β, as shown in Figure 3.

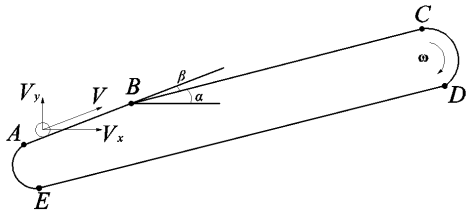

Figure 3. Movement of the rod during separation.

The plum-shaped pulley on the shaft contacts and engages the belt rod as the drive shaft rotates. The impact of the engagement causes elastic deformation of the belt. The deformation is transmitted in the opposite direction of engagement, causing the belt to fluctuate and the rod to vibrate up and down. The engagement process during operation is similar to that of the chain drive. Based on existing research related to chain drives [22–24], the engagement shock process was analyzed. During the working process, the forces on both ends of the rod are symmetrically distributed and the resultant moment is zero, so it was possible to analyze the forces on both sides of the rod at the center of mass. The mechanical model for the engagement of the plum-shaped wheel with the rod was simplified as follows. The belt between the rods is set as a spring of a certain stiffness. The gear teeth are set as a cylinder with a certain mass to impact the rod at a relative speed, as shown in Figure 4.

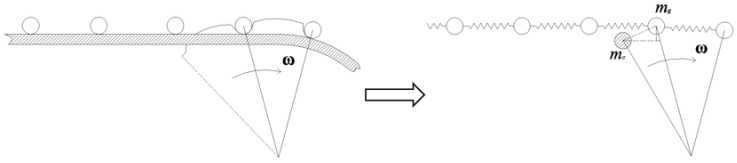

Figure 4. The simplified mechanical model for the engagement of the plum-shaped wheel with the rod.

The total kinetic energy (E_z) at the moment before the engagement is the kinetic energy of the plum-shaped wheel relative to the roller. The collision occurs, causing the relative velocity of the gear teeth to decrease and the velocity of the rod to increase. The

collision is completed when the velocities of the two are equal (v_0). At this point, part of the total kinetic energy is transformed into kinetic energy of the rod and gear teeth, and the other part is transformed into deformation energy (E_b). The total kinetic energy (E_z) can be represented as:

$$E_z = \frac{1}{2} m_g {v_0}^2 + \frac{1}{2} m_c {v_0}^2 + \frac{m_c \rho^2 {v_0}^2}{4{R_0}^2} + E_b = \frac{1}{2} J\omega^2 \quad (1)$$

where the mass of the rod is m_g, the mass of the gear teeth is m_c, the mass of the plum-shaped wheel is M, the rotational inertia is J, the radius of the meshed gear teeth is ρ, and the distance between the center of the plum-shaped wheel circle and the center of the rod is R_0.

The corresponding deformation energy can be obtained by differential transformation of the relationship between the contact deformation and stress, and then substituted into the equations of elastic contact theory and generalized integration. The calculation result is as follows [22]:

$$E_b = \int \sigma ds = \frac{1}{4b} \cdot F^2(\alpha_0 \ln F + 2\beta_0) \quad (2)$$

where σ is the contact stress, s is the contact deformation, b is the contact length, α_0 and β_0 are constants only influenced by the shape and material, and F is the maximum impact force during the engagement, which is calculated as follows:

$$F^2(\alpha_0 \ln F + 2\beta_0) = \frac{2a^2 b m_g \cdot M \cdot \omega^2 \cdot \sin^2\left(\frac{\pi}{6} + \lambda\right)}{2m_g + M} \quad (3)$$

where a is the distance between the bars, ω is the angular velocity, z is the number of teeth of the plum-shaped wheel, and λ is the degree of tooth angle.

From the above equation, it can be seen that the maximum impact force generated by the engagement is related to the shape and material of the plum-shaped wheel and the belt rod. Different speeds also affects the separation process. Each engagement causes the belt to vibrate. This drives the belt-rod up and down in a reciprocating motion. The vibration period (T) is influenced by the rotation speed of the drive shaft.

$$T = \frac{2\pi}{\omega \cdot z} = \frac{\pi}{6\omega} \quad (4)$$

The amplitude of vibration is influenced by the actual installation and belt material, and the amplitude was measured to be about 2 mm according to the actual work with the rod at no load in a previous test. Based on the above analysis, a simple harmonic motion perpendicular to the DE section of the running trajectory of one rod is attached to the whole potato soil separation mechanism driven by the belt pulley in the RecurDyn software. Its equation of motion is 2 × *SIN*(2 × *pi* × *time*/*T*). In this way, the vibration generated by the plum-shaped wheel during the real operation is simulated. The rod whose initial position is at B is selected for analysis of its velocity. v, v_x and v_y indicate the case without vibration and v', v_x' and v_y' indicate the case with additional vibration, as shown in Figure 5.

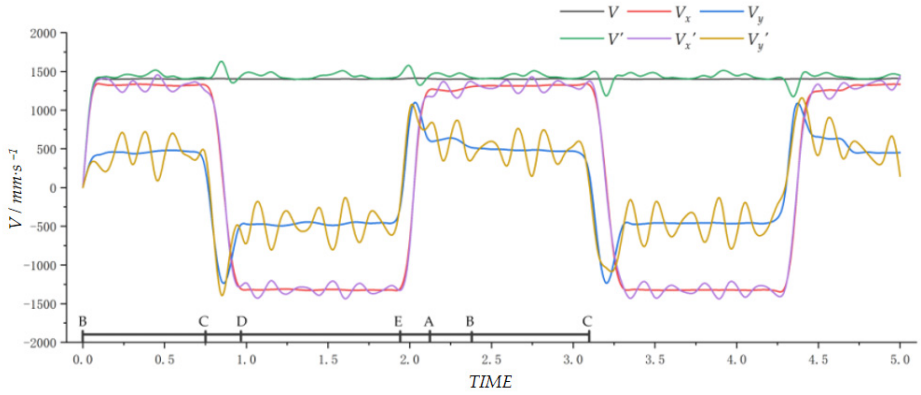

Figure 5. The effect on individual rod speed variation with and without additional vibration.

When the vibration is attached, the speed of the rod fluctuates during the motion. The fluctuation range is around the velocity when no vibration is attached, and the fluctuation range of the component velocity in the horizontal direction (v_x) is small, whereas the component velocity in the vertical direction (v_y) is large. Both have small speed fluctuations during the engagement process. The effect of the presence or absence of additional vibration on the change in rod position is small, and it is numerically slightly more obvious in the y-direction. S S_x and S_y indicate the change of rod position when the vibration is attached to the separation device, as shown in Figure 6.

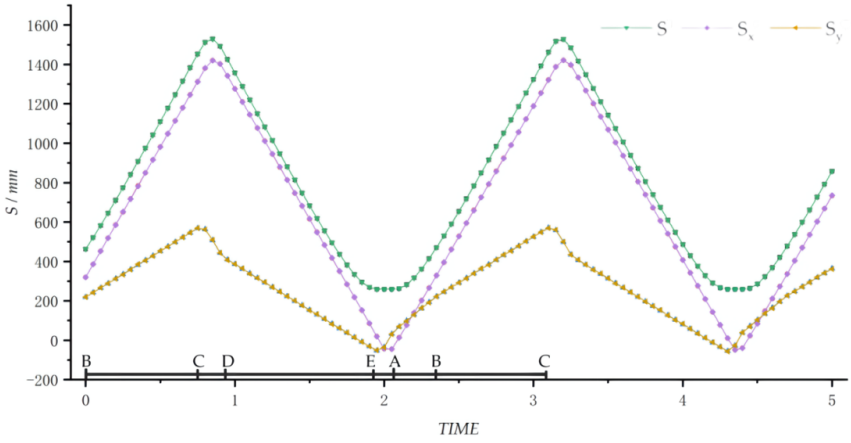

Figure 6. Effect of the presence or absence of additional vibration on the change in rod position.

3.1.2. Analysis of Potato Tubers in the Separation Process

The process of separating and transporting the tubers on the belt-rod can be divided into two parts. The first part with less impact from the rods is in the AB section, where the potato tubers move together with a large amount of fine grain soil. The second part is in the BC section, where fine grain soil is reduced, and the tubers are susceptible to mechanical damage from collisions when moving with rods. Therefore, the motion of the potato tuber in the BC section was analyzed as follows. Taking the frame as a reference, the potato tuber is simplified as a mass point being thrown up and falling on the BC plane. The speed of the tuber when it is thrown up is v_1, and its component velocity in the horizontal and vertical directions is v_{1x} and v_{1y}. The trajectory of the motion from the initial position J through time t_0 to the drop point position P is shown in Figure 7, and the following equation can be obtained.

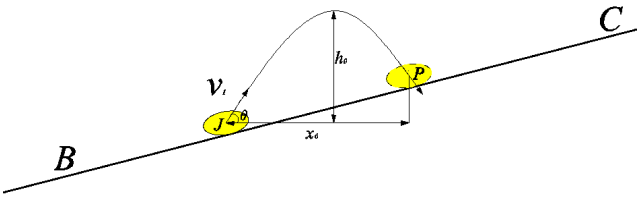

Figure 7. The trajectory of the potato bouncing in one collision on the BC section.

The equation of the velocity and the position of the barycenter of the potato during the separation process as a function of time is described by Equations (5) and (6):

$$\begin{cases} v_{1x} = v_1 \cdot \cos\theta \\ v_{1y} = v_1 \cdot \sin\theta - gt \end{cases} \tag{5}$$

$$\begin{cases} x = v_{1x} \cdot t \\ h = v_1 \cdot \sin\theta \cdot t - \dfrac{1}{2} g t^2 \end{cases} \tag{6}$$

When the vertical direction velocity decreases to 0, h has a maximum of h_0. When t reaches t_0, the horizontal displacement has maximum value of x_0, and the vertical direction displacement is $x_0 \tan\alpha$. The equation is created and solved in terms of the height relationship at point P. The value of t_0 can be obtained as:

$$t_0 = \frac{2v_1 \sin\theta - 2v_1 \cos\theta \tan\alpha}{g} \tag{7}$$

The damage to the potato tuber is influenced by the time and height of the collision, which in turn, is related to the initial velocity (v_1) and the angle between the belt-rod and the horizontal direction. The initial speed before the collision varies depending on the driving situation.

3.1.3. Analysis of Soil in the Separation Process

1. Fine grain soil

During the working process, most of the fine grain soil is screened in the AB section, and in this stage, it can be roughly divided into two categories. One is the lower soil, which is the first to be acted upon by the rods after entering the separation mechanism and flies out of the gaps to achieve sieving. We analyzed the simplified model for this case as shown in Figure 8. The soil grain with mass m_t is in contact with the rod before it is about to finish screening when it is subjected to the force of the other soil-potato mixture as well as the rod. At this point, it is approximated that the velocity is equal to the linear velocity of the belt-rod. After a sufficiently short instant (Δt) the soil grain is no longer in contact with the rod and other mixtures. We assume that the contact force varies uniformly in Δt. Thereafter the soil grain is subjected to an oblique projectile motion with only gravity, which has an initial velocity resolved in the horizontal (v_{fx}) and vertical directions (v_{fy}). The relationship equation can be obtained, as shown in Equations (8) and (9):

$$\int_0^{\Delta t} F_{tx} \cdot dt = \frac{1}{2} F_{tx} \cdot \Delta t \tag{8}$$

$$\begin{cases} v_{fx} = v \cdot \cos(\alpha + \beta) + \dfrac{F_{tx} + F_g \cos\gamma}{2m_t} \cdot \Delta t \\ v_{fy} = -v \cdot \sin(\alpha + \beta) + \dfrac{F_{ty} + 2m_t g - F_g \sin\gamma}{2m_t} \cdot \Delta t \end{cases} \tag{9}$$

where F_{tx} and F_{ty} are the combined forces of the other mixtures on this soil particle in the horizontal and vertical directions. F_g is the support force of the rod on the particle, and γ is the angle of the support force with the horizontal direction. Based on a hypothetical

condition, there is an example provided in Equation (8) for calculating F_{tx}, F_{ty} and F_g in the same way. All of the grains experience different forces depending on their location. Soil grains that are not in contact with the rods before separation are no longer subjected to the action of the rod, and the analysis process is similar to that described above.

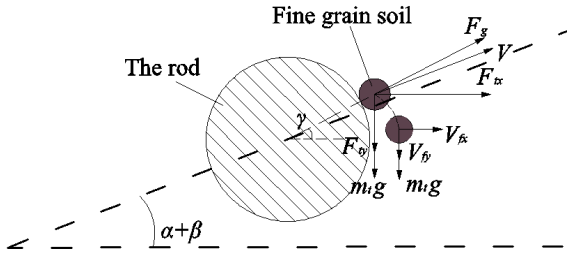

Figure 8. Analysis of the lower soil layer when it was screened.

The other category is the upper soil that does not come into direct contact with the rod when entering the belt-rod. The model was simplified and analyzed as shown in Figure 9. The soil grain with mass m_t' is in a position close to the surface when entering the separation mechanism. At this moment. it is subject to the force of gravity as well as other soil-potato mixtures, and the velocity is v_2. The soil grain moves with the separation mechanism, and after t_1, gradually with the same velocity v as the rod, as described in Equation (10). It then moves downward as the soil grains below continued to decrease. When in contact with the rod, it behaves similarly to the first category of grains.

$$\begin{cases} v \cdot \cos(\alpha + \beta) = v_2 \cdot \cos\delta + \dfrac{F_{tx}{}'}{m_t{}'} \cdot t_1 \\ v \cdot \sin(\alpha + \beta) = -v_2 \cdot \sin\delta + \dfrac{F_{ty}{}' - m_t{}' g}{m_t{}'} \cdot t_1 \end{cases} \tag{10}$$

In Equation (10), δ is the angle between the velocity (v_2) and the horizontal direction. F_{tx}' and F_{ty}' are the components in the horizontal and vertical directions of the resultant forces from the other potato-soil mixtures. As the separation proceeds, the partial force in the vertical direction gradually decreases. F_{tx}' and F_{ty}' are affected by the soil content on the separation mechanism, which means that it is affected by the harvesting speed of the machine.

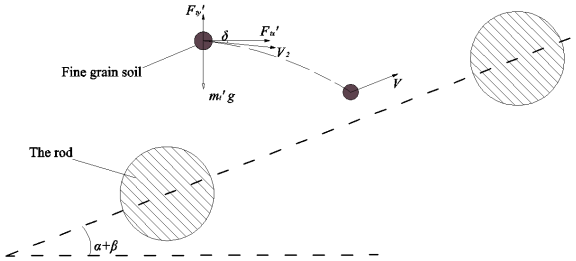

Figure 9. Analysis of the upper soil layer when it is screened.

Combining the two cases, the separation effect of fine grain soil on the AB section is influenced by the belt-rod linear velocity, the harvester forward speed, and the angle between the belt-rod and horizontal direction.

2. Soil block

Most of the soil blocks in the BC section are larger in size than the gap between the rods, and they are broken after contact with the belt-rod. After entering the separation device, the soil blocks have the same motion in both the forward harvesting direction and the belt-rod linear velocity direction. It is believed that there is no relative motion between the soil blocks and the rods other than collision and breakage. When collisional crushing

occurs, the soil block with velocity v_T collides with the rod with velocity v_g. The mechanical energy lost in the process is transformed into the deformation energy that causes the soil block to break, as shown in Figure 10.

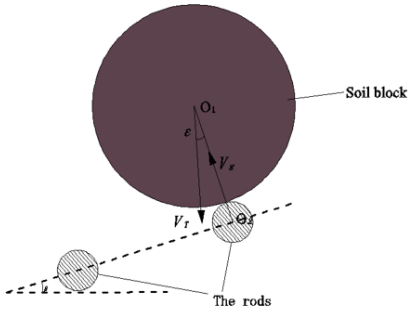

Figure 10. Analysis of the soil block when it is screened.

The velocity v_T of the soil block is resolved into a tangential velocity v_{Tt} along the direction of the belt-rod and a normal velocity v_{Tn} perpendicular to the belt-rod. The direction of v_g is the positive direction, O_1O_2 is the projection axis, and the following equation is obtained from the conservation of momentum and the definition of the coefficient of restitution k:

$$\begin{cases} m_g \cdot v_g - m_T v_{tn} = m_T u_{Tn} + m_g u_g \\ k = \dfrac{u_g - u_{Tn}}{v_g + v_{Tn}} \end{cases} \tag{11}$$

where m_T is the mass of the block, ε is the acute angle between v_T and v_g, u_T is the velocity of the block after the collision, whose component velocities are u_{Tn} and u_{Tt}, and u_g is the velocity of the rod after the collision. The kinetic energy lost in the collision is converted to the energy E' of the soil block broken [25] in this collision. According to the kinetic energy theorem combined with the value of the collision recovery coefficient, the following equations can be obtained:

$$\begin{cases} u_{Tn} = -v_T \cdot \cos\varepsilon + (1-k)\dfrac{m_g}{m_T + m_g}(v_g + v_T) \\ u_{Tt} = v_T \cdot \sin\varepsilon \\ u_g = v_g + (k-1)\dfrac{m_T}{m_T + m_g}(v_g + v_T) \end{cases} \tag{12}$$

$$\Delta E = \frac{1}{2} m_T ({v_{Tn}}^2 - {u_{Tn}}^2) + \frac{1}{2} m_g (v_g^2 - u_g^2) = 0.4872 \cdot \frac{m_T m_g}{(m_T + m_g)} (v_{Tn} + v_g)^2 = l\pi R^3 c = E' \tag{13}$$

where l is a coefficient less than 1, R is the radius of the large soil block, and c is the soil bond strength.

Combined with the above analysis, the fragmentation of the soil block is related to its own physical characteristics, but also to the driving situation of the separation mechanism and the harvester forward speed.

According to the above analysis, the movement and force changes of potato tubers, fine grain soil and soil blocks in the separator are mainly affected by the belt-rod angle, belt-rod linear velocity and harvester forward speed. The setting of the belt-rod linear velocity is related to the actual harvesting environment, but it should not exceed 1.85 m/s [21], and the harvester forward speed should generally be slightly less than the belt-rod linear velocity. According to the available studies [26–28] and design requirements, the belt-rod linear velocity is 1.20–1.80 m/s, and the harvester forward speed is 0.60–1.40 m/s. When the angle of the belt-rod is less than 10 degrees, it affects the assembly of the whole machine and reduces the performance of soil separation. When the angle is higher than

40 degrees, the potato tuber returns, which is not conducive to backward transportation and tuber-soil separation. Therefore, the angle of the belt-rod should be set in the range 10–40°.

3.2. Simulation Tests of Tuber-Soil Separating Operation

3.2.1. Construction of the MBD Model

A multi-body dynamics model was developed using RecurDyn software. The frame and drive shaft of the belt-rod type potato soil separating device were simplified in SolidWorks and imported into RecurDyn. We modeled the flexible belt in RecurDyn and added rods, pulleys, drive wheels and the other required components. To improve the modeling efficiency and reduce the calculation required for the simulation, the plum-shaped wheels on the drive shaft and the slight vibration caused by the engagement were simplified to pulleys drive and a simple harmonic motion perpendicular to the direction of the belt-rod motion was added for the whole separation device in conjunction with the analysis in Section 3.1. The material of the bars, frame and other components was set to steel. Constraints need to be added to each body to determine the movement of the belt-rod. These mainly included the fixed joints between the rods and the belts, the contact between the pulleys and the belts, the drive revolving joints between the drive pulleys and the frame, and the revolving joints between the other pulleys and the frame.

3.2.2. Construction of the DEM Model

A discrete element model of the post-excavation soil-potato mixture was developed in EDEM. The percentage of soil and tubers within the range of two potato plants was measured in the field by hand digging. Based on this result, the potato-soil mixture before the separation operation can be divided into potato tubers, soil blocks, and fine grain soil.

After measuring and counting the shape and size of the soil-potato mixture in the field, it was determined that the potato particles were ellipsoidal in shape with sizes of 78 mm in the long-axis direction and 48 mm in the short-axis direction. The amount of fine grain soil was determined by the total mass of soil excavated from the field, and the radius of the particles was increased to 7 mm to reduce the amount of calculation as appropriate. The excavated soil blocks can be divided into two approximate types: columnar soil blocks and plate-like soil blocks. The dimensions measured in the field were combined with existing studies [29,30] to create the model of the soil blocks. The particle replacement and additional Bonding model were applied, as shown in Figure 11.

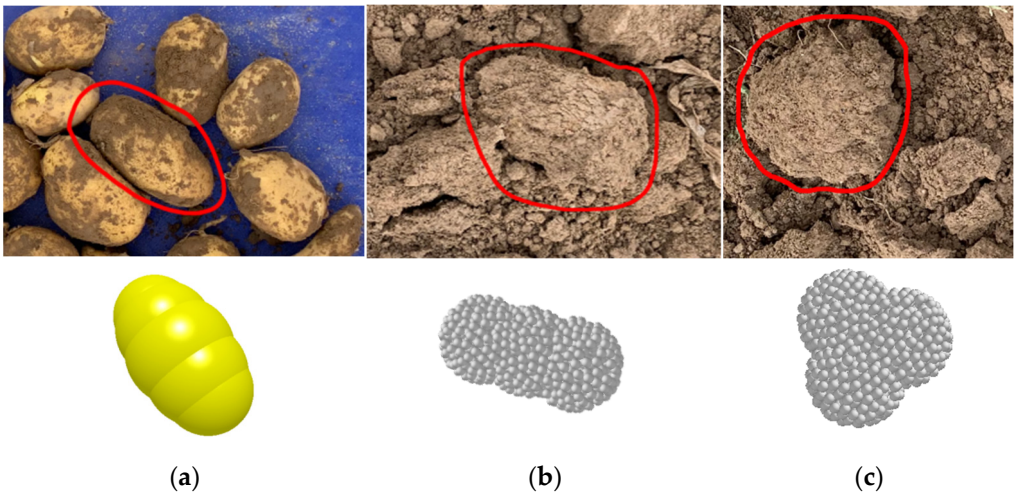

(**a**) (**b**) (**c**)

Figure 11. Potato tubers, soil blocks and their DEM models: (**a**) potato tubers in the field and the DEM model; (**b**) columnar soil block and the DEM model; (**c**) plate-like soil block and the DEM model.

We built a steel soil bin. The particles were generated in the soil bin in batches with a layer of fine grain soil particles, a layer of potato tubers and soil blocks, then a layer of fine grain soil particles. Modeling of potato-soil mixtures was then performed. Based on previous research and experience [17,31], the Hertz–Mindlin contact model with an additional Bonding model were selected for the simulation, whose parameters are shown in Table 1.

Table 1. Discrete element simulation parameters.

Parameter	Value	Parameter	Value
Coefficient of Restitution between the potato	0.668 [a]	Coefficient of Restitution between potato and soil	0.060 [b]
Coefficient of Static Friction between the potato	0.452 [b]	Coefficient of Static Friction between potato and soil	0.500 [b]
Coefficient of Rolling Friction between the potato	0.024 [b]	Coefficient of Rolling Friction between potato and soil	0.010 [b]
Coefficient of Restitution between the soil	0.484 [c]	Coefficient of Restitution between potato and rod	0.634 [a]
Coefficient of Static Friction between the soil	0.549 [c]	Coefficient of Static Friction between potato and rod	0.445 [b]
Coefficient of Rolling Friction between the soil	0.203 [c]	Coefficient of Rolling Friction between potato and rod	0.269 [b]
Coefficient of Restitution between rod and soil	0.160 [b]	Normal Stiffness per unit area between the soil	3.00×10^6 [c]
Coefficient of Restitution between rod and soil	0.600 [b]	Shear Stiffness per unit area between the soil	1.61×10^6 [c]
Coefficient of Rolling Friction between rod and soil	0.350 [b]	Critical Normal Stress between the soil	2.25×10^5 [c]
		Critical Shear Stress between the soil	1.50×10^5 [c]

Note: [a]-by actual measurement, [b]-by reference, [c]-by parameter calibration.

3.2.3. DEM-MBD Coupling Simulation

The rods and the frame in RecurDyn that were directly in contact with the discrete element particles were imported into the EDEM software in the form of Wall files, and the joint simulation calculation between EDEM and RecurDyn was realized through the coupling interface. The particles of the tuber-soil mixture to be separated were located in front of the belt-rod. The result of the completed separation can be observed in the receiving bin behind the separating device. The time step in EDEM was 7e-5 s, and the target save interval was 0.01 s. The step in Recurdyn was 700. The construction of the DEM-MBD coupling simulation model is shown in Figure 12.

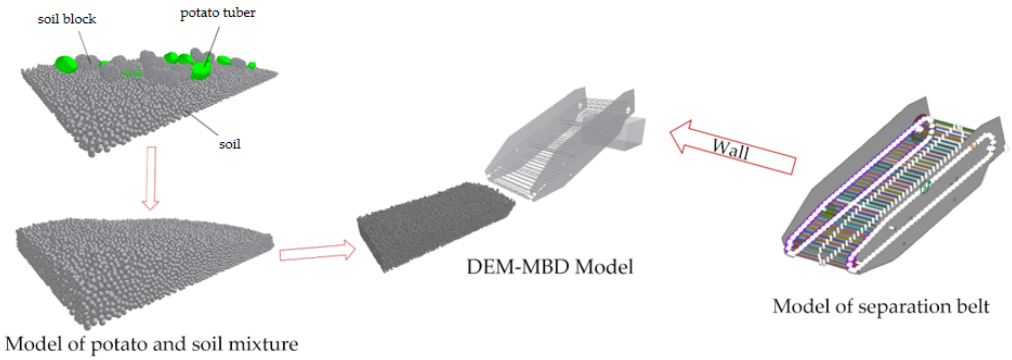

Figure 12. The construction of DEM-MBD coupling simulation model.

3.3. Single-Factor Test and Test Index

According to the previous theoretical analysis and in order to investigate the effect of each factor on the separation characteristics, single-factor tests were conducted at the levels of 10.0°, 17.5°, 25.0°, 32.5° and 40.0° for the belt rod angle, at 1.20, 1.35, 1.50, 1.65 and 1.80 m/s for the belt rod linear velocity, and at 0.60, 0.80, 1.00, 1.20 and 1.40 m/s for the harvester forward speed.

The effect on potato damage and soil clearing capability was studied. The data of potato blocks and soil particles at each moment of the simulation process were obtained by EDEM analyst. The maximum value of the force on all tubers was used to estimate the damage to the potato. The tubers are damaged when the force exceeds 200 N [32]. The soil

removal rates (mass ratio) and the bonding of soil blocks breakage rates (ratio of number) over time were used as the capability of soil clearing.

3.4. Box–Behnken Design Test

After determining the range of influencing factors based on the results of the single-factor test, a three-factor, three-level BBD test was conducted on the potato-soil separation process based on the coupled DEM-MBD model. The belt-rod angle (X_1), belt-rod linear velocity (X_2), and harvest forward velocity (X_3) were selected as the influencing factors. The coefficient of force on the potato (Y_1) and soil removal rate (Y_2) were used as the response values, where Y_1 is the sum of the average forces applied to all potato tubers at each moment during the whole separation process. Y_2 is the ratio of the removed soil mass to the initial soil mass, as shown in Table 2.

The testing program was derived according to the Box–Behnken design principle, and the central group was set to be 5 groups of 17 groups. The results of the experiment were then analyzed by multiple regression with Design-Expert software to determine the model of the regression equation. The interactions between the factors and the effects were then studied by using response surface analysis. This was used as the basis for parameter optimization of the separating belt-rod and validated with field trials.

Table 2. Test factors and levels.

Levels	Factors		
	Angle of Belt-Rod X_1	**Linear Velocity of Belt-Rod X_2**	**Harvest Forward Velocity X_3**
−1	17.5°	1.20 m/s	0.80 m/s
0	25.0°	1.35 m/s	1.00 m/s
1	32.5°	1.50 m/s	1.20 m/s

4. Results

4.1. Single-Factor Test Results

The effect of the belt-rod angle on the separation effect is shown in Figure 13. When the angle of the belt rod increased from 10° to 40°, the peak values of the maximum force on the potato tubers were 55.55 N, 81.68 N, 82.99 N, 119.54 N, 149.41 N, respectively. The soil removal rates were 96.87%, 97.67%, 98.21%, 98.45%, 98.45%, and the bonding breakage rates of soil blocks were 39.24%, 42.87%, 46.47%, 58.19% and 65.20%, respectively.

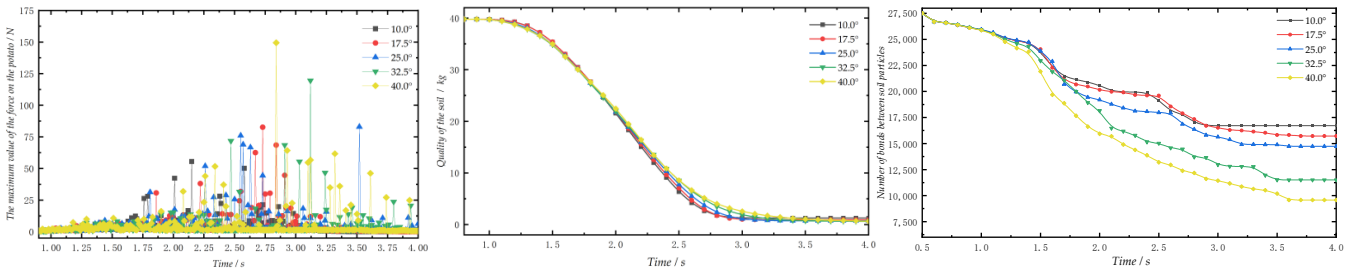

(**a**) (**b**) (**c**)

Figure 13. The effect of the belt-rod angle on the separation: (**a**) peak values of the maximum force on tubers; (**b**) soil removal rates; and (**c**) bonding breakage rates.

The effect of belt-rod linear velocity on the separation effect is shown in Figure 14. With the increase in the linear velocity of the belt-rod, the peak of the maximum force on the potato block was 118.75 N, 109.72 N, 80.99 N, 87.81 N, 66.41 N; the soil removal rate was 98.55%, 98.11%, 98.21%, 97.81%, 97.57%; the bonding breakage rate of the soil block was 45.11%, 43.82%, 46.47%, 44.78%, and 48.44%, respectively.

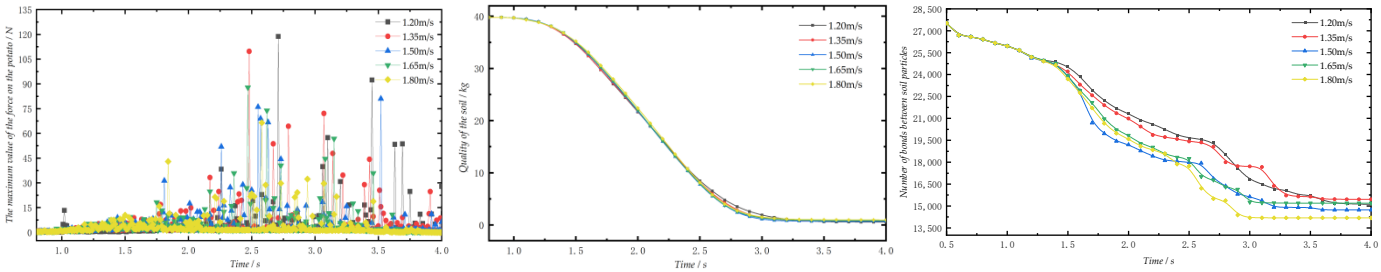

(**a**) (**b**) (**c**)

Figure 14. The effect of belt-rod linear velocity on the separation: (**a**) peak values of the maximum force on tubers; (**b**) soil removal rates; and (**c**) bonding breakage rates.

The effect of harvest forward velocity on the separation effect is shown in Figure 15. With the increase in harvesting forward velocity, the peak force on potato tubers was 87.70 N, 83.47 N, 80.99 N, 90.45 N, 74.64 N; the soil removal rate was 98.63%, 98.41%, 98.21%, 96.61%, 95.50%; the bonding breakage rate of the soil blocks was 43.34%, 45.20%, 46.47%, 45.53%, and 46.42%, respectively.

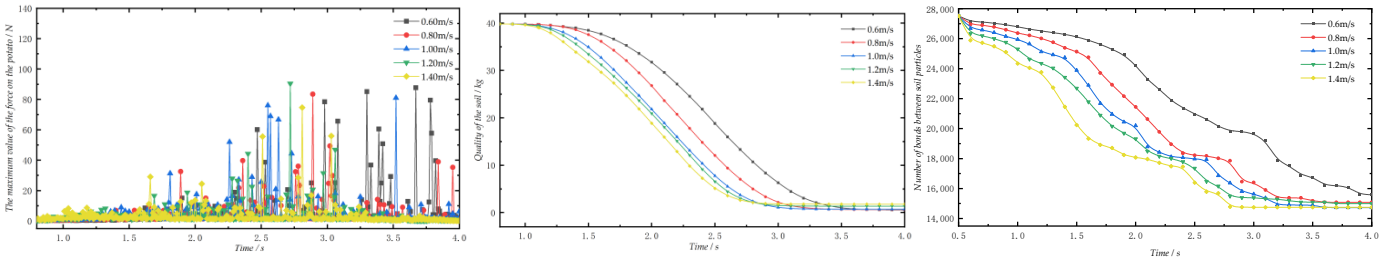

(**a**) (**b**) (**c**)

Figure 15. The effect of harvest forward velocity on the separation. (**a**) The peak values of the maximum force on tubers; (**b**) The soil removal rates; (**c**) The bonding breakage rates.

According to the above test results, the angle range of the belt-rod was selected to be 17.5–32.5°, the linear velocity range of the belt-rod was 1.20–1.50 m/s, and the harvesting forward velocity range was 0.80–1.20 m/s for subsequent tests.

4.2. The Result of Box–Behnken Design Test

4.2.1. Results and Regression Analysis

The results of the experiment are shown in Table 3, and the multiple regression and fitting analysis were performed by Design-Expert software. Multiple regression equations were established for the three independent variables belt-rod angle X_1, belt-rod linear velocity X_2, and harvesting forward velocity X_3 with the response values coefficient of force on the potato Y_1 and soil clearing rate Y_2.

$$\begin{aligned} Y_1 = &-2986.27 + 82.24X_1 + 2234.63X_2 + 2277.43X_3 \\ &-49.06X_1X_2 - 5.43X_1X_3 - 1524.92X_2X_3 \end{aligned} \quad (14)$$

$$\begin{aligned} Y_2 = &78.41 - 0.36X_1 + 23.39X_2 + 20.90X_3 + 0.06X_1X_2 \\ &+ 0.19X_1X_3 - 13.85X_2X_3 - 4.80{X_2}^2 - 4.52{X_3}^2 \end{aligned} \quad (15)$$

Table 3. Experimental program and results.

No.	Factors			Response Values	
	X_1	X_2	X_3	Y_1	Y_2/%
1	1	0	−1	589.22	98.79
2	0	0	0	518.01	98.33
3	0	−1	1	648.43	98.37
4	−1	1	0	412.48	97.68
5	0	1	1	416.23	97.00
6	1	0	1	572.74	98.56
7	−1	0	−1	448.00	98.68
8	1	−1	0	774.18	99.00
9	0	0	0	475.99	98.36
10	0	0	0	536.49	98.36
11	−1	0	1	464.13	97.29
12	−1	−1	0	471.53	98.46
13	0	0	0	496.36	98.36
14	0	1	−1	441.22	98.60
15	1	1	0	494.33	98.48
16	0	0	0	480.98	98.39
17	0	−1	−1	490.42	98.31

The analysis of variance results are shown in Table 4. It can be seen that the model of Y_1 to X_1, X_2 and X_3 is 2FI, and the model of Y_2 to X_1, X_2 and X_3 is quadratic. The p values of both models are less than 0.05, indicating that the two regression equations are highly significant. The p values of the Lack of Fit term are greater than 0.05, which are not significant, indicating a good fit of the equation. The R^2 for Y_1 and Y_2 are 0.913 and 0.998, respectively, indicating that more than 90% of the response values could be explained by the regression model. In summary, the models can be used for analysis and optimization. From the results of the analysis, the coefficient of force on the potato Y_1 was significantly affected by X_1, X_2, whereas X_3 was not significant. The interactions X_1X_2 and X_2X_3 had a significant effect, whereas X_1X_3 had a non-significant effect. The effect degree of each influencing factor on Y_1 was X_1, X_2, and X_3 in descending order. The soil clearing rate Y_2 was significantly affected by X_1, X_2, X_3, the interaction terms X_1X_2, X_2X_3, X_1X_3, and the squared terms X_1^2, X_2^2, X_3^2. The effect degree of each influencing factor on Y_2 is X_3, X_1, and X_2 in descending order.

Table 4. Variance analysis of regression equations.

Source	Y_1 (2FI)				Source	Y_2 (Quadratic)			
	Sum of Squares	df	F Value	p Value		Sum of Squares	df	F Value	p Value
Model	121,400.00	6	17.49	<0.0001	Model	4.22	9	407.48	<0.0001
X_1	50,299.30	1	43.47	<0.0001	X_1	0.93	1	810.67	<0.0001
X_2	48,095.72	1	41.57	<0.0001	X_2	0.71	1	616.78	<0.0001
X_3	2200.24	1	1.90	0.198	X_3	1.25	1	1090.14	<0.0001
X_1X_2	12,187.23	1	10.53	0.0088	X_1X_2	0.02	1	14.43	0.0067
X_1X_3	265.84	1	0.23	0.642	X_1X_3	0.34	1	295.57	<0.0001
X_2X_3	8371.34	1	7.23	0.0227	X_2X_3	0.69	1	599.82	<0.0001
					X_1^2	0.10	1	86.21	<0.0001
					X_2^2	0.05	1	42.72	0.0003
					X_3^2	0.14	1	119.68	<0.0001
Residual	11,570.92	10			Residual	0.0081	7		
Lack of Fit	8975.58	6	2.31	0.2192	Lack of Fit	0.0067	3	6.56	0.0504
Pure Error	2595.34	4			Pure Error	0.0014	4		
Cor Total	133,000	16			Cor Total	4.23	16		

The effect of the interaction term on the coefficient of force on the potato Y_1 is shown in Figure 16. Figure 16a shows that the force on the potato increases with the increase in the angle of the belt-rod X_1, and it decreases with the increase of the line velocity of the belt-rod X_2. Figure 16b indicates that as the angle of the belt-rod X_1 increases, the greater the force on the potato, and as the harvesting forward velocity X_3 increases, the greater the force on the potato. Figure 16c indicates that the force on the potato increases with the increase in the line speed of the belt-rod X_2, the force on the potato increases with the increase in the harvest forward velocity X_3 at the low level of X_2, and the opposite occurs at the high level of X_2.

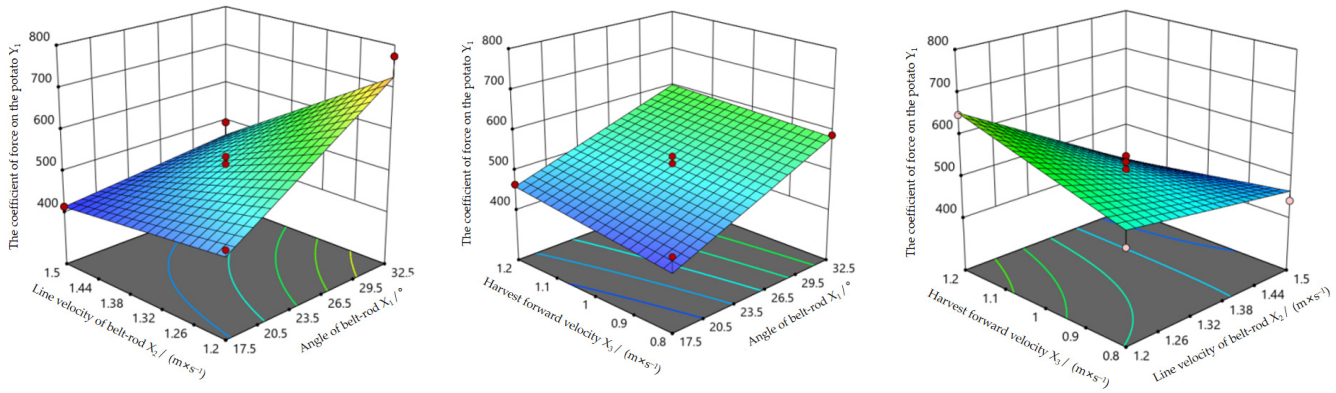

(**a**) (**b**) (**c**)

Figure 16. Response surface of interaction factors to coefficient of force on the potato Y_1: (**a**) response surface under factors X_1 and X_2; (**b**) response surface under factors X_1 and X_3; and (**c**) response surface under factors X_2 and X_3.

The effect of the interaction term on the soil clearing rate Y_2 is shown in Figure 17. Figure 17a shows that the soil clearing rate decreases with the increasing belt-rod velocity X_2, which increases with increasing belt-rod angle X_1. The effect of clearing soil is better when the belt-rod angle is larger and the line velocity is lower. Figure 17b shows that the soil clearing rate decreases with increasing harvesting forward velocity X_3, and the changing trend is small at a larger belt-rod angle. The soil clearing rate increases with increasing belt-rod angle X_1 and the trend is greater when the harvesting velocity is higher. Figure 17c indicates that the soil clearing rate decreases significantly when both harvest forward velocity X_3 and belt-rod line velocity are at high levels.

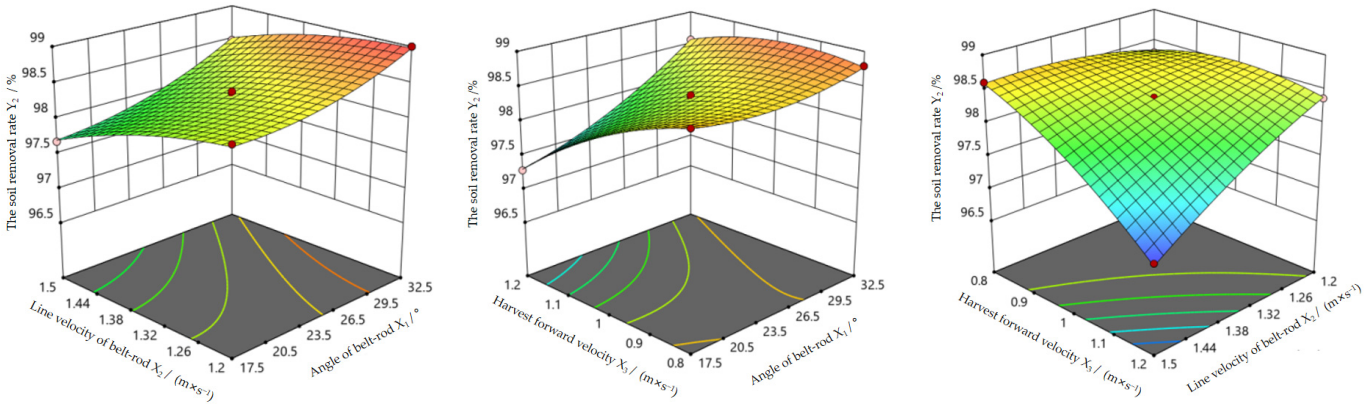

(**a**) (**b**) (**c**)

Figure 17. Response surface of interaction factors to soil clearing rate Y_2: (**a**) response surface under factors X_1 and X_2; (**b**) response surface under factors X_1 and X_3; and (**c**) response surface under factors X_2 and X_3.

4.2.2. Parameter Optimization

According to the results of the above analysis, to further improve the potato-soil separation capacity of the belt-rod separation mechanism, the minimum coefficient of force on the potato Y_1 and the highest soil clearing rate Y_2 were required in the separation operation. Taking these as the optimization index, the optimal parameters can be found.

$$\begin{cases} \min\ Y_1(X_1, X_2, X_3) \\ \max\ Y_2(X_1, X_2, X_3) \end{cases} \tag{16}$$

$$\begin{cases} 17.5^\circ \leqslant X_1 \leqslant 32.5^\circ \\ 1.20\ \leqslant X_2 \leqslant 1.50 \\ 0.80\ \leqslant X_3 \leqslant 1.20 \end{cases} \tag{17}$$

Using the Design-Expert software, the optimal combinations of parameters that satisfy the constraints can be solved as follows. With the belt-rod angle of 17.5°, belt-rod line velocity of 1.37 m/s and harvesting forward velocity of 0.8 m/s, the coefficient of force on the potato Y_1 is predicted to be 412.48 and the soil clearing rate Y_2 is 98.68%. This set of parameters was substituted into the DEM-MBD model and the simulation was repeated three times to obtain values for the coefficient of force on the potato blocks of 405.51, 407.31, and 408.32, and the clearing rates were 98.65%, 98.67%, and 98.65%. The peak values of the maximum force on the potato during separation were 64.58 N, 69.04 N, and 62.43 N, and the mass ratios of potato to soil after completing the separation were 1.73, 1.75, and 1.73, respectively.

4.2.3. Field Test Verification

The small-scale self-propelled potato combine harvester developed by the team was used to conduct field trials in October 2021 in Huining County, Gansu Province, as shown in Figure 18. The potato variety harvested was LongShu NO.7. planted in a single row within one ridge. The height of the ridge was 200 mm, the bottom width of the ridge was 500 mm, and the plant spacing was 35 mm. During the test, the subsequent mechanisms of the combine harvester, such as the scraper chain lifting mechanism, were kept at a standstill, and field harvesting was performed with only the belt-rod type potato soil separation device in operation. The quality of the potato tubers and soil after sieving by the potato-soil separation device were measured separately, and the tubers were assessed for damage or broken skin. The field harvesting operations were carried out according to the optimized parameters and the results were recorded.

Figure 18. Field trial of the small-scale self-propelled potato combine harvester.

With 10 potato plants harvested each time, three tests were conducted in the field to produce an average result. Since the mass of soil at the time of entering the separation device could not be measured during actual excavation, the mass ratio of potato to the soil after separation was used as a reference for the separation effect. The results are shown in Table 5. After careful observation of the separated tubers, the average value of the broken skin rate for the three tests was 0.59%, and no tuber was found with significant internal damage. Most of the residue after tuber-soil separation consisted of soil blocks. The mean value of error between the simulation test and field test results is 3.81%, which verifies the validity and reliability of the simulation model.

Table 5. The mass ratio of potato to soil for simulation tests and field tests.

Test Number	Simulation Results	Field Tests	Deviation
1	1.73	1.69	2.42%
2	1.75	1.68	4.10%
3	1.73	1.65	4.92%

5. Discussion

The objective of this research on potato-soil separation is to reduce the forces on the potato and to ensure the effectiveness of soil removal during the separation operation.

When the potato is on the belt-rod in the separation operation, the tuber is thrown up and then falls on the rod, and the kinetic energy is converted into potential energy and then into kinetic energy by the action of the rod. The tuber collides with the elastic deformation and accumulates energy, after which the energy is gradually converted into kinetic energy to achieve the next throw [11]. However, if the energy accumulated during the collision is greater than the limit of elastic deformation, there will be some energy transferred to plastic deformation of the potato. That is, it will cause damage to the potato tuber. The larger angle increases the force on the potatoes [17]. From the simulation results, it was found that when the angle is 40°, not all the potato tubers can be transported to the next mechanism, and the phenomenon of backflow occurs. The force on the potato block increases more obviously with the line speed of the belt rod when the angle of the belt rod is large. The reason for this may be that the larger angle causes the potato to be prone to sliding downward and coming into contact with the rods more frequently. As the belt-rod line velocity increases, the potato-soil mixtures are transported faster and the potato tubers are subjected to less force [33]. However, when the line velocity is low, increasing the forward speed of harvesting will lead to increased forces on the potato blocks. This also suggests that the length of time the tuber is in contact with the rods may be the main factor determining the force on the potato.

The soil sieving process is stochastic, with particles at different locations subjected to slight variations in forces from the soil-potato mixture and rod bars, which is related to the quality of the soil-potato mixture obtained at different harvesting speeds. When the angle of the belt-rod is increased, the fine grain soil can be screened out of the gap faster, and the soil removal effect is improved. The faster the belt-rod line velocity, the faster the soil is being sieved, but it also leads to a shorter time to sieve the soil on the separation device, resulting in poor soil clearing [17]. The energy required to break the soil block is mainly determined by the shape of the block and its characteristics, such as moisture content [25]. The breakage energy transformed by the collision is related to the initial velocity before the collision in addition to the mass of the belt rod and the soil mass. The vibration and breakage of the soil blocks is determined by a combination of different belt-rod line velocities and the total mass of the soil-potato mixtures on the separation mechanism. The increase in belt-rod line velocity affects the vibration of the rods and facilitates the breaking of soil blocks. In addition, to ensure that the potatoes are as little damaged as possible during the first separation in the combine harvester, the tubers can be protected by keeping some of the soil in place, because after the first potato soil separation, this part of the

soil will also pass through a series of mechanisms with secondary soil removal capabilities such as the potato-haulm separation device and lifting mechanism. This also ensures the soil removal capability of the combine harvester.

It was found that the percentage of soil in the field trial harvest was higher than in the simulation. One possible reason is the neglect in the simulation model of belts that can hinder the sieving of soil. A very small portion of the soil falls on the belts and is transported upwards during field harvesting, and this portion cannot be completely screened. Another possible reason is that the effect of the excavation shovel was not considered when the simulation test was conducted, with the result that the form of the soil-potato mixture entering the separation belt-rod during the simulation experiment differed from the actual situation. In future studies, the simulation model will be further optimized and the process of digging and separating could be simulated by considering the excavation shovel and the belt-rod type separation mechanism working together to reduce the error with the field harvest results.

6. Conclusions

(1) The potato-soil separation characteristics in a combine harvester were analyzed. The movement of the belt-rod and the engagement vibration during the separation, the movement of the potato tubers during the separation process, the screening of the fine grain soil and the breakage of the soil blocks were investigated. It was found that the main factors affecting the potato-soil separation characteristics of the belt-rod type include the belt-rod angle, belt-rod linear velocity and forward harvest velocity. A simulation model based on DEM-MBD coupling was constructed and a series of simulation tests were conducted.

(2) Single-factor simulation tests were conducted, and with the increase in the belt-rod angle, the higher the peak of the maximum force on the potato, and the better the effect of soil breakage. An increase in the belt-rod line velocity resulted in a smaller peak in the maximum force on the potato and a decrease in the soil removal rate but it was more favorable to soil block breakage. With the increase of the harvest forward velocity, the soil removal rate was reduced and the soil crushing effect was improved.

(3) Based on the results of the single-factor experiments, a three-factor, three-level Box–Behnken test was conducted with the coefficient of force on the potato and soil clearing rate as response indicators. The effects and interactions between the factors on the corresponding indicators were determined. A set of optimal parameters was derived based on the established regression equation: a belt-rod angle of 17.5°, a belt-rod line velocity of 1.37 m/s, and a harvest forward velocity of 0.80 m/s. According to the field validation tests, the error between the simulation model and the real harvest was 3.81%, which verified the reliability of the simulation model and demonstrated that the optimal parameters could meet the need to reduce potato tuber damage in the first potato-soil separation stage of the potato combine harvester.

Author Contributions: Conceptualization, Y.L. and F.W.; methodology, Y.L., F.G., H.Y. and F.W.; software, Y.L. and H.Y.; validation, H.Y., B.W. and J.F.; formal analysis, Y.L. and F.G.; investigation, Y.L., B.W. and J.F.; resources, F.W., Z.H. and B.W.; data curation, B.W. and J.F.; writing—original draft preparation, Y.L. and H.Y.; writing—review and editing, Y.L., H.Y. and F.G.; supervision, Z.H. and F.W.; project administration, Y.L.; funding acquisition, Z.H. All authors have read and agreed to the published version of the manuscript.

Funding: This research was funded by the Natural Science Foundation of Jiangsu Province, grant number BK20201124; the Central Public Interest Scientific Institution Basal Research Fund, grant number S202110-02, S202110-03.

Institutional Review Board Statement: Not applicable.

Informed Consent Statement: Not applicable.

Data Availability Statement: The data presented in this study are available on demand from the first author at l598658625@163.com.

Conflicts of Interest: The authors declare no conflict of interest.

References

1. Liu, J. General situation of potato planting and measures to improve benefits in China. *Agric. Eng.* **2021**, *11*, 142–144.
2. Dongre, A.U.; Battase, R.; Dudhale, S.; Patil, V.R.; Chavan, D. Development of potato harvesting model. *Int. Res. J. Eng. Technol. (IRJET)* **2017**, *4*, 1567–1570.
3. Sibirev, A.; Aksenov, A.; Dorokhov, A.; Ponomarev, A. Comparative study of the force action of harvester work tools on potato tubers. *Res. Agric. Eng.* **2019**, *65*, 85–90.
4. Kuyu, C.G.; Tola, Y.B.; Abdi, G.G. Study on post-harvest quantitative and qualitative losses of potato tubers from two different road access districts of Jimma zone, South West Ethiopia. *Heliyon* **2019**, *5*, e2272.
5. Yang, R.; Yang, H.; Shang, S.; Ni, Z.; Liu, Z.; Guo, D. Design and experiment of vertical circular separating and conveying device for potato combine harvester. *Trans. Chin. Soc. Agric. Eng.* **2018**, *34*, 10–18.
6. Wei, H.; Zhang, J.; Yang, X.; Huang, X.; Dai, L.; Sun, G.; Liu, X. Improved design and test of 4UFD-1400 type potato combine harvester. *Trans. Chin. Soc. Agric. Eng.* **2014**, *30*, 12–17.
7. Bayboboev, N.G.; Muxamedov, J.M.; Goyipov, U.G.; Akbarov, S.B. Design of Small Potato Diggers. In *IOP Conference Series: Earth and Environmental Science*; IOP Publishing: Bristol, UK, 2022; p. 12080.
8. Duskulov, A.A.; Makhmudov, K.S. Improved potato digger. In *IOP Conference Series: Earth and Environmental Science*; IOP Publishing: Bristol, UK, 2021; p. 12055.
9. Al-Dosary, N.M.N. Potato harvester performance on tuber damage at the eastern of Saudi Arabia. *Agric. Eng. Int. CIGR J.* **2016**, *18*, 32–42.
10. Zhou, J.; Yang, S.; Li, M.; Chen, Z.; Zhou, J.; Gao, Z.; Chen, J. Design and experiment of a self-propelled crawler-potato garvester for hilly and mountainous areas. *INMATEH Agric. Eng.* **2021**, *64*, 151–158. https://doi.org/10.35633/inmateh-64-14.
11. Lv, J.; Yang, X.; Lv, Y.; Li, Z.; Li, J.; Du, C.; Analysis and Experiment of Poatao Damage in process of Lifting and Separating Potato Excavator. *Trans. Chin. Soc. Agric. Mach.* **2020**, *51*, 103–113.
12. Wu, B.; Huang, T.; Qiu, X.; Zuo, T.; Wang, X.; Xie, F. Design and Experimental Study of Potato-Soil Separation Device for Sticky Soils Condition. *Appl. Sci.* **2021**, *11*, 10959. https://doi.org/10.3390/app112210959.
13. Zhao, H.; Huang, Y.; Liu, Z.; Liu, W.; Zheng, Z. Applications of discrete element method in the research of agricultural machinery: A review. *Agriculture* **2021**, *11*, 425.
14. Wang, S.; Yu, Z.; Zhang, W. Study on the modeling method of sunflower seed particles based on the discrete element method. *Comput. Electron. Agric.* **2022**, *198*, 107012.
15. Byum, J.H.; Nam, J.S.; Choe, J.S.; Inoue, E.; Okayasu, T.; Kim, D.C. Analysis of the separating performance of a card cleaner for pepper harvester using EDEM software. *Fac. Agric. Kyushu Univ.* **2018**, *63*, 347–354.
16. Li, J.; Jiang, X.; Ma, Y.; Tong, J.; Hu, B. Bionic design of a potato digging shovel with drag reduction based on the discrete element method (DEM) in clay soil. *Appl. Sci.* **2020**, *10*, 7096.
17. Wei, Z.; Su, G.; Li, X.; Wang, F.; Sun, C.; Meng, P. Parameter Optimization and Test of Potato Harvester Wavy Sieve Based on EDEM. *Trans. Chin. Soc. Agric. Mach.* **2020**, *51*, 109–122.
18. Park, D.; Lee, C.G.; Park, H.; Baek, S.H.; Rhee, J.Y. Discrete Element Method Analysis of the Impact Forces on a Garlic Bulb by the Roller of a Garlic Harvester. *J. Biosyst. Eng.* **2019**, *44*, 208–217. https://doi.org/10.1007/s42853-019-00031-z.
19. Li, B.; Gao, G. Research on Parameter Optimization of Potato Soil Transportation Separation Mechanism. In Proceedings of the 2019 2nd World Conference on Mechanical Engineering and Intelligent Manufacturing (WCMEIM), Shanghai, China, 22–24 November 2019; IEEE: Piscataway, NJ, USA, 2019; pp. 147–150.
20. Gao, G.; Xie, H. Numerical Analysis and Simulation of Potato Soil Separation Mechanism Based on EDEM. *J. Agric. Mech. Res.* **2019**, *41*, 15–21.
21. Wei, H.; Wang, D.; Lian, W.; Shao, S.; Yang, X.; Huang, X. Development of 4UFD-1400 type potato combine harvester. *Trans. Chin. Soc. Agric. Eng. (Trans. CSAE)* **2013**, *29*, 11–17.
22. Wang, J.; Cui, L. Calculation on the Impact Loading of oil-filed Roller Chain Drives. *China Pet. Mach.* **1989**, *17*, 19–26.
23. Xu, L. Theoretical and Experimental Study on the Dynamics of Roller Chain Drive System. Doctor Thesis, Tianjing University, Tianjin, China, 2010.
24. Lu, J. Design and Test of Online Dynamic Balance Detection System for Multi-roller Structure of Combine Harvester. Master's Thesis, Jiangsu University, Zhenjiang, China, 2019.
25. Lv, J.; Sun, H.; Dui, H.; Peng, M.; Yu, J. Design and Experiment on Conveyor Separation Device of Potato Digger under Heavy Soil Condition. *Trans. Chin. Soc. Agric. Mach.* **2017**, *48*, 146–155.
26. Zhang, Z.; Wang, H.; Li, Y.; Yang, X.; Issa, I.B.R.A.H.I.M.; Zhang, Z. Design and Experiment of Multi-stage Separation Buffer Potato Harvester. *Trans. Chin. Soc. Agric. Mach.* **2021**, *52*, 96–109.
27. Wan, E.; Shang, S.; Wang, D.; He, X.; Liu, X. Design and Test of Tractive Potato Combined Harvester. *J. Agric. Mech. Res.* **2019**, *41*, 80–84.

28. Wang, B.; Hu, L.; Hu, Z.; Tian, L.; Ji,F.; Ma, B. Damage mechanism study of chain-lever elevator sweet potato harvester. *J. China Agric. Univ.* **2014**, *19*, 174–180.
29. Hao, J.; Long, S.; Li, J.; Ma, Z.; Zhao, X.; Zhao, J.; Li, H. Effect of granular ruler in discrete element model of sandy loam fluidity in Ma yam planting field. *Trans. Chin. Soc. Agric. Eng.* **2020**, *36*, 56–64.
30. Wang, Y. Simulation Analysis of Structure and Effect of the Subsoiler Based on DEM. Master's Thesis, Jilin Agricultural University, Changchun, China, 2014.
31. Ji, L.; Xie, H.; Yang, H.; Wei, H.; Yan, J.; Shen, H. Simulation analysis of potato drysoil cleaning device based on EDEM-Recurdyn coupling. *J. Chin. Agric. Mech.* **2021**, *42*, 109–115.
32. Xie, S.; Wang, C.; Deng, W. Experimental study on collision acceleration and damage characteristics of potato. *J. Food Process. Eng.* **2020**, *43*, e13457. https://doi.org/10.1111/jfpe.13457.
33. Shen, H.; Wang, B.; Hu, L.; Wang, Ge.; Ji, L.; Shen, G.; Wu, T. Design of potato connecting and conveying mechanism for 4UZL-1 type sweet potato combine harvester. *Trans. Chin. Soc. Agric. Eng.* **2020**, *36*, 9–17.